The Effect of Two-Step Austempering on Abrasion Wear Characteristics of the Ductile Cast Iron

C. S. Wadageri, R. V. Kurahatti, Dayanand M. Goudar, Vijaykumar Hiremath, and V. Auradi

Abstract This paper focuses on the effect of two-step austempering on abrasion wear characteristics of the ductile cast iron. The single-step (conventional) and two-step austempering were employed for the samples. There were four treatments. For all samples, austenitization at 900 °C was done. The first treatment comprised of conventional austempering at 400 °C. The second one consisted of conventional austempering at 320 °C. The third one consisted of austempering at 400 °C followed by austempering at 320 °C. The fourth one comprised of austempering at 320 °C followed by austempering at 400 °C. The results showed that samples with two-step austempered at 320 °C followed by 400 °C exhibited enhanced abrasion resistance. The reason for this behavior is discussed considering the microstructure parameters.

Keywords Ductile iron · Two-step austempering · Abrasion resistance

1 Introduction

Recent studies [1–3] have shown that ductile iron can be utilized in applications requiring sudden impact loading and wear resistance. Examples of uses are automotive parts like transmission gears and crankshafts, agricultural implements and

C. S. Wadageri
Department of Mechanical Engineering, Maratha Mandal Engineering College, Belagavi 591 113, Karnataka, India

R. V. Kurahatti (✉)
Department of Mechanical Engineering, Basaveshwar Engineering College, Bagalkot, Karnataka 587 102, India
e-mail: rajukurahatti@gmail.com

D. M. Goudar
Department of Mechanical Engineering, Tontadarya Collge of Engineering, Gadag, Karnataka 582 101, India

V. Hiremath · V. Auradi
Department of Mechanical Engineering, Siddaganga Institute of Technology, Tumakuru, Karnataka 572 103, India

defense equipments. Austempered ductile iron (ADI) parts used are frequently subjected to abrasive wear. Most studies [3–6] focused on adhesive and abrasive wear performance of ADI. Zimba et al. [2] inferred that ADI could be used as alternate material for earth moving equipment. Zhou and Zhou [4] and Shepperson et al. [5] investigated the rolling wear characteristics of ductile iron. Studies on fatigue performance of ductile iron are found in the literature [3].

The wear of ADI gears was investigated by Magalhaes and co-workers [6]. The effect of superiority of casting on the abrasion performance was studied by several researchers. The effect of graphite nodule shape and size on the sliding wear of ductile iron was studied by Hatate et al. [7]. The authors noted that the change in nodule shape, i.e., from spheroid to flake, was the main cause for lower wear loss in ADI. Very few studies threw a light on the role of austempering temperature and time on the wear resistance of ductile iron. Zhou and Zhou [4] studied the wear (on oiled surface) performance of ductile iron and showed that wear resistance initially reduced and eventually increased substantially with increased austempering temperature. Other studies [8, 9] confirmed the beneficial effects of microstructure parameters on the abrasive wear behavior.

This paper compares the effect of conventional and two-step austempering temperature and time on the abrasion resistance of ductile iron. The microstructure details and their effect on the wear behavior are considered.

2 Details of Experiment

2.1 Materials

The ingredients of the ductile iron in weight percentage were C (3.48%), Si (2.4%) Mn (0.31%) Cu (0.03%) P (0.01%) S (0.01%) and Mg (0.05%).

2.2 Heat Treatment Procedures

The following heat treatments were carried out on ADI samples. Figure 1 shows the procedures schematically.

- Austenitization at 900 °C was done for all samples.
- Sample 1: Conventional austemepering (CA-1) at 400 °C for 150 min
- Sample 2: Conventional austempering (CA-2) at 320 °C for 150 min
- Sample 3: Two-step austempering (TSA-1), i.e., austempering at 400 °C for 30 min followed by austempering at 320 °C for 120 min
- Sample 4: Two-step austempering (TSA-2), i.e., austempering at 320 °C for 30 min followed by austempering at 400 °C for 120 min
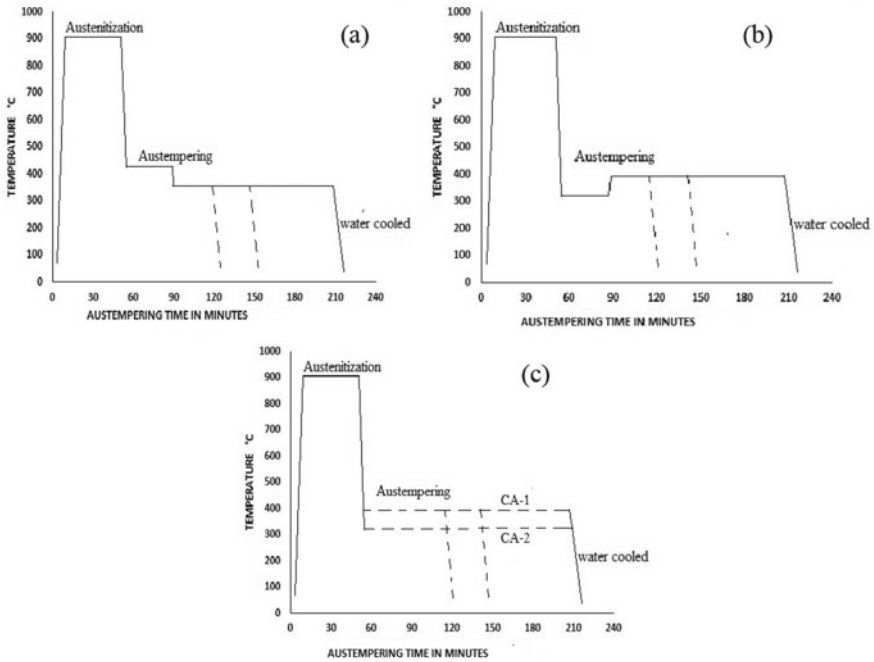
Fig. 1 Schematic diagrams of two-step austempering **a**, **b** and conventional austempering processes **c**

2.3 Quantitative Analysis

The contents (volume percentage) of microconstituents like austenite and carbon in austenite were determined using the X-ray diffractometer, as per ASTM E975-84 [10, 11].

2.4 Abrasion Wear Test

Figure 2 shows the abrasion test setup. The abrasion test was conducted according to ASTM standard G132-96. A load of 65 N was used. The disk rotated at 22 rpm; it traveled a distance of 13 m at 0.04 m/s. 0.1 mg accuracy weighing equipment was used. The sample weights before and after the wearing tests were noted and weight loss was determined. Three readings were noted and the average value was used for reporting. Rockwell hardness test (C scale) was utilized to determine the hardness of the worn-out surfaces. Vickers hardness test was used for testing the hardness of untreated and heat-treated samples.

Fig. 2 Abrasion test setup
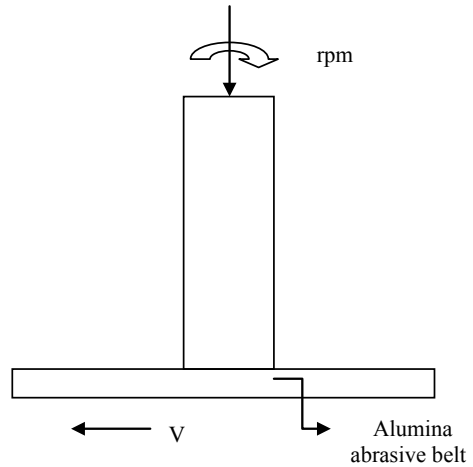
3   Results and discussion

3.1   *Microstructural details*

Table 1 shows the microstructural details such as contents of austenite (Xγ), carbon in austenite (Cγ) and austenitic carbon (XγCγ) as obtained from heat treatment procedures mentioned. It is clear that more austenitic carbon content (XγCγ) was obtained from TSA-2 (400 °C, 150 min) process. The mechanism of microstructure development is found in the literature [12]. Table 2 shows the weight loss details of the tested samples.

Table 1   Microstructural details of the samples

Samples	Austenite Xγ (vol. %)	Carbon in austenite Cγ (vol. %)	Total carbon in matrix, XγCγ (vol. %)
TSA-1 (320 °C, 60 min)	0.3	1.89	0.56
TSA-1 (320 °C, 90 min)	0.28	1.8	0.5
TSA-1(320 °C,150 min)	0.16	1.7	0.27
TSA-2 (400 °C, 60 min)	0.19	1.85	0.35
TSA-2 (400 °C, 90 min)	0.35	1.95	0.68
TSA-2 (400 °C, 150 min)	0.38	2.01	0.76
CA-1 (400 °C, 150 min)	0.15	1.7	0.25
CA-2 (320 °C, 150 min)	0.36	1.96	0.71

Table 2 Weight loss details of the samples

| Sample	Weight loss (milligrams, mg)
Untreated ductile iron	85.2
TSA-1 (320 °C, 60 min)	79.3
TSA-1 (320 °C, 90 min)	79.2
TSA-1 (320 °C, 150 min)	74
TSA-2 (400 °C, 60 min)	78.1
TSA-2 (400 °C, 90 min)	77.8
TSA-2 (400 °C, 150 min)	70
CA-1 (400 °C, 150 min)	76.2
CA-2 (320 °C, 150 min)	74.9

Table 3 Hardness and tensile properties of ADIs (austempering time: 150 min)

Austempering temperature	Hardness (VHN)		Yield strength (MPa)		Tensile strength (MPa)		Elongation (%)	
Untreated ductile iron	280		550		880		1.8	
	CA	TSA	CA	TSA	CA	TSA	CA	TSA
320 °C	480	435	822	855	1092	1126	2.1	2.2
400 °C	310	410	618	811	976	1076	5.2	2.6

Table 3 shows the effect of conventional and two-step austempering on the hardness and tensile properties of samples. It is observed that as the austempering temperature increased, hardness and strengths were decreased. This was due to the fact that austenite and ferrite become coarser at higher temperature (400 °C). The coarse grains formed result in the remarkable decrease in strengths. This is only true for conventional and two-step austempering (400 °C). The strength values are higher in CA and TSA processes (320 °C). This is due to grain size effect. The finer grains at 320 °C result in higher tensile properties (Hall–Petch equation). Relatively higher strengths and lower ductility were observed in TSA processed materials.

3.2   Abrasion properties

Numerous workers [3–6] concluded that it was the austempering temperature and time that is main reason for modification of microstructure The modified microstructure ultimately determines the wear behavior of the samples. This has become true in our study. By TSA-2 (400 °C, 150 min) process, the microstructure constituents as observed in Table 1, i.e., higher austenite $X\gamma$ (vol.%) and higher total carbon in matrix, $X\gamma C\gamma$ (vol.%) were obtained. The hardness of ADIs has drastically improved
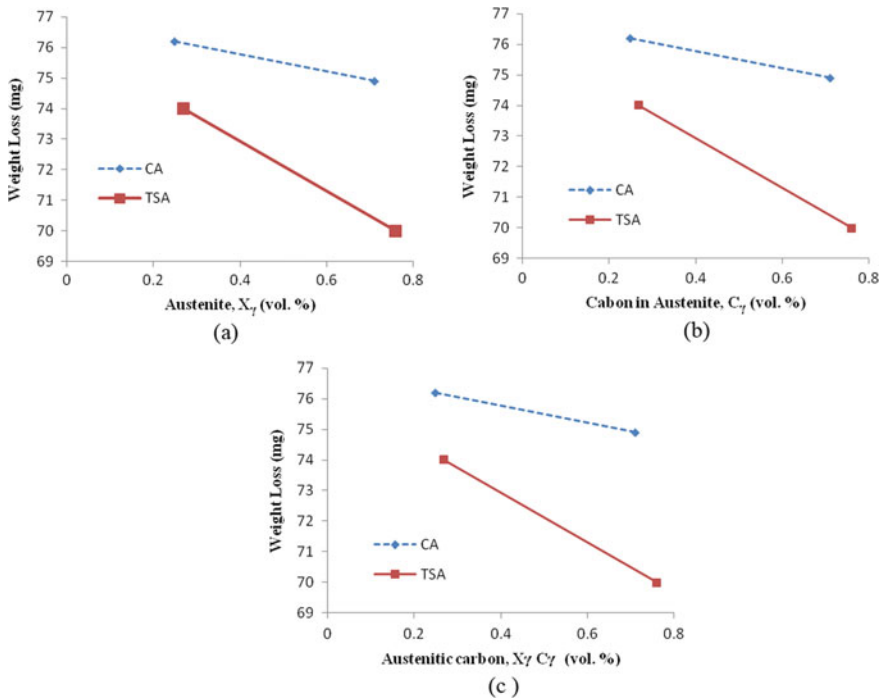
Fig. 3 Weight loss versus vol. % of austenite (Xγ) **a** weight loss versus vol. % of carbon content in austenite (Cγ) **b** weight loss versus vol. % of austenitic carbon (XγCγ) **c** (austempering time: 150 min)

due to this microstructure evolution. The improved abrasion wear resistance may be attributed to the enhanced hardness and tensile properties of the materials (Table 3).

From Fig. 3a, it is clear that the wear loss increased as the austenite volume fraction increased. It is further noticed that for same volume fraction of austenite, TSA-2 (400 °C, 150 min) samples exhibited lesser weight loss. The austenite with FCC structure is soft and capable of undergoing higher work hardening. The BCC ferrite is not so. So considering this argument, the more austenite should have been the cause for more wear loss. TSA-2 processes have created more austenite than the TSA-1 processes. On the contrary, the wear loss appeared lesser as compared to TSA-1 processes. This behavior was attributed to work hardening of the austenite during the abrading process. The work hardening phenomenon could be confirmed by the hardness readings obtained after the abrasion test (Table 4).

Figure 3b, c clearly shows that the carbon content in austenite and austenitic carbon has identical effect on weight loss of materials. Normally diffusion of carbon atoms in austenite is more at higher temperature. This results in carbon enriched austenite. The carbon atoms form the interstitial solid solution within FCC austenite lattice. The strength of austenite phase thereby increases. The strengthened matrix naturally gives rise to improved abrasion resistance.

Table 4 Hardness of samples prior to and after abrasion test

Samples	Hardness prior to wear (HRC)	Worn surface hardness (HRC)
TSA-1 (320 °C, 60 min)	19	30.4
TSA-1 (320 °C, 90 min)	23	36.4
TSA-1 (320 °C, 150 min)	38	45
TSA-2 (400 °C, 60 min)	35	36.5
TSA-2 (400 °C, 90 min)	38.5	41.2
TSA-2 (400 °C, 150 min)	47	48.5
CA-1 (400 °C, 150 min)	39.5	45
CA-2 (320 °C, 150 min)	22.5	30.4

It becomes clear from Table 4 that hardness of the worn surfaces has increased. There is more increment in hardness in TSA-2 samples particularly in TSA-2 (400 °C, 150 min). Gundlach, Janowak [13] and other researchers [4, 5] indicated the hardness increase and they concluded that after the wearing, work hardening and the strain-induced martensite were the cause for this behavior [14].

Optical examination of worn surfaces of ADIs exhibits that surface morphology (Fig. 4) consisted of typical shallow scars and grooves. The worn surfaces showed a look of semi-polished metallographic surface consisting of coarse interwoven abrasive grooves. It seems that the grooves and scars may have been formed by hard abrasive particles that exist in belt while undergoing abrasion test. Deep grooves, shear lips existed near the abraded areas. This occurrence was more evident in TSA-2 samples. This shear lips broke finally and formed the abrasion debris.
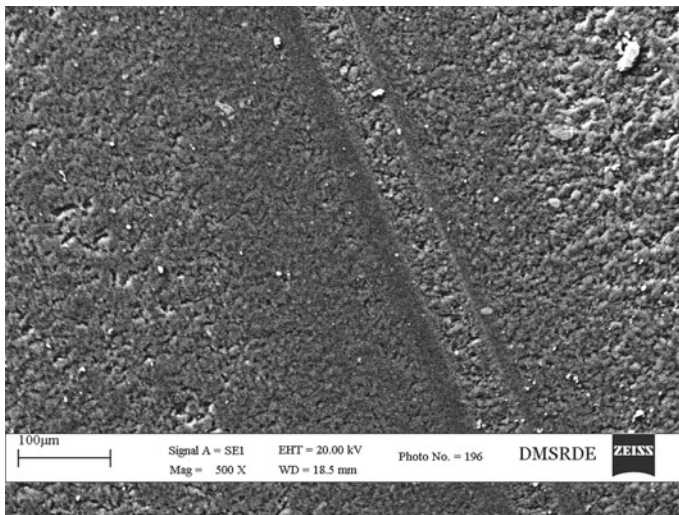
Fig. 4 Worn surface morphology of two-step austempered ductile iron sample (400 °C, 150 min)

4   Conclusion

Based on the present study, the following conclusions were made.

1. Due to two-step process, the microstructure of ductile iron sample consisted of fine ferrite and more austenitic carbon. This microstructure was the reason for enhanced hardness and strength values in the samples.
2. The materials processed by TSA-2 (400 °C, 150 min) exhibited lowest wear loss of 70 mg compared to as-cast sample 85.2 mg. This was due to higher austempering temperature and time.
3. Higher worn surface hardness was observed for material having greater wear resistance.

References

1. Zimba, J., Samandi, M., Yu, D., Chandra, T., Navara, E., & Simbi, D. J. (2004). *Materials and Design, 25*(5), 431–438.
2. Zimba, J., Simbi, D. J., & Navar, E. (2003). *Cement Concrete Composite, 25*(6), 643–649.
3. Dommarco, R. C., & Salvande, J. D. (2003). *Wear, 254*(3–4), 230–236.
4. Zhou, W.-S., & Zhou, Q.-D. (1993). *Wear, 162–164,* 696–702.
5. Shepperson, S., & Allen, C. (1988). *Wear, 121,* 271–287.
6. L. Magalh˜aes, J. Seabra, Wear 215 (1–2) (1998) 237–246.
7. Hatate, M., Shiota, T., Takahashi, N., & Shimizu, K. (2001). *Wear, 251*(1–2), 885–889.
8. Larsen-Basse, J. (1990). *Scripta Metallurgica et Materialia, 24*(5), 821–826.
9. K.-H. Zum Gahr, in: K.C. Ludema, et al. (Eds.), Wear of Materials, ASME, New York, 1979, pp. 266–274.
10. Cullity, B. D. (2001). *Elements of X-ray diffraction* (3rd ed.). Upper Saddle River: Prentice Hall.
11. Rouns, T. N., & Rundman, K. B. (1987). Constitution of austempered ductile iron and kinetics of austempering (retroactive coverage). *AFS Trans, 95,* 851–874.
12. Yang, J., & Putatunda, S. K. (2004). *Materials and Design, 25*(3), 219–230.
13. Gundlach, R. B., & Janowak, J. F. (1983). *AFS Trans., 94,* 377–388.
14. Garin, J. L., & Mannheim, R. L. (2003). *Journal of Materials Processing Technology, 143–144,* 347–351.